Supplemental Materials for

Cancer associated mesothelial cells promote ovarian cancer chemoresistance through paracrine osteopontin signaling

Jin Qian, Bauer L. LeSavage, Kelsea M. Hubka, Chenkai Ma, Suchitra Natarajan, Joshua T. Eggold, Yiren Xiao, Katherine C. Fuh, Venkatesh Krishnan, Annika Enejder, Sarah C. Heilshorn, Oliver Dorigo, Erinn B. Rankin*

Supplemental Methods

Cell culture

LP9 and LP3 mesothelial cells were obtained from the Coriell Institute. LP9, LP3 and primary CAMs and HPMCs were cultured in media containing 40% Ham's F-12, 40% Medium M199 (Thermo Fisher Scientific, Cat# 11150-067), 20% FBS. Primary HGSOC cell line OC8 was a generous gift from Dr. Weiping Zou (1), and was cultured in RPMI 1640 media supplemented with 10% FBS. Primary HPMCs and CAOV3 cell line was a generous gift from Dr. Katherine C. Fuh (2). Ovarian cancer cell lines OVCAR8, CAOV3 and SNU119 were cultured in DMEM supplemented with 10% FBS (2). In addition, cells were tested upon receipt for viability, cell morphology, and the presence of Mycoplasma and viruses. All cells were cultured at 37°C supplied with 5% CO2.

Primary mesothelial cell isolation

Ascites-derived primary CAM1 and CAM2 cells were isolated from the malignant ascites of ovarian cancer patients (Supplemental Table 1) at Stanford under a Stanford University institutional review board–approved protocol with informed consent. As previous described (*20*), after brief centrifugation at low speed, ascites cell pellets were seeded at high density and cultured on Poly-L-lysine (Sigma Aldrich) covered surface in culture medium until cell confluence was reached. Under this culture condition, mesothelial cells were enriched without contamination of other cell types (3). Primary HPMCs were derived from omentum of patients with benign disease as described previously (2). All primary mesothelial cells were used for studies within six passages.

Primary mesothelial cell staining

Primary mesothelial cells were seeded into 8-well chamber slides (Thermo Fisher Scientific), and fixed in 4% paraformaldehyde for 20 minutes. Cells were blocked in serum-free protein block

(Dako) for 10 minutes at room temperature, and then stained in primary antibody solution at 4°C overnight. The primary antibodies included antibodies against Calretinin (Invitrogen, 1:50), Vimentin (Thermo Fisher Scientific, 1:50), Cytokeratin 8 (Abcam, 1:100), FSP1 (Novus Biologicals, 1:100), CD31 (Abcam, 1:20), FITC-CD45 (Thermo Fisher Scientific, 1:20) and EpCAM (Abcam, 1:50). The following day, secondary antibodies conjugated with Alexa Fluor Dyes (Thermo Fisher Scientific, 1:500) were incubated for 1 hour at room temperature, except for FITC-CD45 stained samples. DAPI (Sigma Aldrich) was used for nuclear counterstaining at 0.1 μg/ml, and representative images were taken under the Leica SPE microscope to confirm mesothelial cell purity.

In vivo cisplatin response study

To establish co-injected xenograft models, 1×10^6 cancer cells were mixed with or without 1×10^6 mesothelial cells immediately before injection in 50% Matrigel solution (Corning) in PBS. Cell suspensions were injected subcutaneously into the left flank of 8-12 week-old female *Rag2*$^{-/-}$ *IL2rg*$^{-/-}$ mice. To examine the influence of LP9 co-culture on cancer cell chemoresistance, cancer cells were monocultured or co-cultured with LP9 in vitro as described for 2 weeks and then cancer cells were injected subcutaneously into the left flank of 8-12 week-old female *Rag2*$^{-/-}$*IL2rg*$^{-/-}$ mice at 1×10^6 cell number in the 50% Matrigel solution. Tumor incidence varied among injection groups, and the percentage of mice with palpable tumors within each group is as shown in Figure 3. For LP9 CM preincubation of tumor cells, cancer cells were preincubated in control medium or LP9 CM with control antibody or an anti-OPN antibody at 20 μg/ml for 10 days, and then injected subcutaneously into the left flank of 8-12 week-old female *Rag2*$^{-/-}$*IL2rg*$^{-/-}$ mice at 0.5×10^6 cell number in the 50% Matrigel solution. When the tumors reached an average volume of 100-160 mm^3, these mice were randomized into each group. For cisplatin treatment, cisplatin was

administered intraperitoneally at 5 mg/kg every three days for a total of three treatments as indicated. Tumor size was measured every 2 or 3 days using calipers and tumor volumes were calculated using the formula: tumor volume (mm^3) = (length x $width^2$)/2. Mice with morbidities as determined by the Stanford veterinary staff (example skin lesions) were excluded from tumor growth and weight analysis.

OPN aptamer treatment in the ID8 tumor model

OPN apatamer and mutant aptamer were synthesized as previously reported (4). To test the in vivo therapeutic potential of OPN aptamer, 2 x 10^6 ID8 cells were injected to 8-12 week-old female C57BL/6J mice intraperitoneally. Ten days after cancer cell injection, mice were treated with either cisplatin with mutant aptamer, or OPN aptamer, or the combination of cisplatin with OPN aptamer. Cisplatin was administrated intraperitoneally at 3 mg/kg every three days for a total of three consecutive injections. OPN aptamer or mutant aptamer was administrated intraperitoneally at 100nmol/kg every day until the end of experiment. Tumor number and weight, ascites volume and omentum weight was measured at the end of experiment.

For ID8 ascites cells, total cell suspension was deposited by cytospin onto glass slides. Cells were then fixed in 10% formalin for 20 mins, and blocked. Cells were permeabilized with 0.2% Tween-20 in PBS, blocked in serum-free protein block (Dako) for 10 minutes at room temperature, and then stained in primary antibody (Goat Anti-osteopontin Antibody, Novus Biologicals, 1:100; Rabbit Anti-calretinin Antibody, Invitrogen, 1:50) solution at room temperature for 1 hour. After washing, anti-rabbit or anti-goat secondary antibodies conjugated with Alexa Fluor Dyes were added for 30 minutes at room temperature. DAPI (Sigma Aldrich) was used for nuclear counterstaining at 0.1 μg/ml and images were taken under Leica SPE

microscope.

In vivo limiting dilution assay

For the LP9 co-injected model, cancer cells (cell number 100, 1000, or 10000) were mixed with or without LP9 cells at 1:1 ratio right before injection, and cell suspensions were injected subcutaneously into the left flank of 8-12 week-old female *Rag2*$^{-/-}$*IL2rg*$^{-/-}$ mice in 50% Matrigel solution (Corning) in PBS. For the LP9 co-culture model, cancer cells were monocultured or co-cultured with LP9 in vitro as described for 2 weeks and cancer cells (cell number 100, 1000 or 10000) were injected subcutaneously into the left flank of 8-12 week-old female *Rag2*$^{-/-}$*IL2rg*$^{-/-}$ mice in the 50% Matrigel solution. Tumor appearance were closely monitored, and around 1 month after inoculation, mice were sacrificed to check tumor formation on the injected site.

Indirect co-culture of cancer cells with mesothelial cells

Ovarian cancer cells were seeded into the bottom chamber of 75 mm co-culture dishes (Corning, Cat# 3419) at 4-6 × 10^4 cells. After 8 hours, 12 × 10^4 LP9, LP3 or primary CAMs were seeded onto the upper insert of 0.4 μm pore size. The inserts allowed for interaction between the two cell types without physical contact. The co-culture system was incubated at 37°C for a total of 7 days and then cancer cells were passaged and/or checked for phenotypic changes. For examination of HPMCs after co-culture with ovarian cancer cells, HPMCs were grown on the bottom, while cancer cells were grown on the upper insert of 0.4 μm pore size for a total of 7 days.

Generation of conditioned medium and cell treatments

Cells were cultured at 80-90% confluence in 1% FBS culture medium. After 72 hours, the conditioned media from cultures were transferred to Amicon Ultra-15 Centrifugal Filter units (Millipore) with 10 KDa molecular weight cut-off through a 0.45-mm syringe filter and centrifuged at 4,000 rcf for 30 minutes. The conditioned media was concentrated to 20-fold

concentrated medium by adding fresh medium. The concentrated medium was then mixed at 1:1 ratio with basal medium for utilization in further studies. For some experiments, Proteinase K was added to CM as previously reported (1). For OPN inhibition experiments, the anti-OPN neutralizing antibody (R&D) was added at the concentration of 20 μg/ml to the cell media. For CD44 and integrin receptors blocking experiments, the anti-CD44 blocking antibody (Bioxcell) and RGD (Abcam) was added at the concentration of 10 μg/ml. For TGFβ1 related experiments, human recombinant TGFβ1 (Peprotech) dissolved in 4 mM HCL was applied at the concentration of 10 ng/ml for 3 days. SB431542 (Millipore) was added at the concentration of 10 μM in cell media as previously reported (5).

Cell viability assay

Ovarian cancer cell lines were seeded in 96-well plates after treatment. Cells were then treated with cisplatin, carboplatin or paclitaxel at two drug concentrations that span IC50. After 2-3 days, cell viability assays were performed using CellTiter-Glo Viability Assay (Promega) or CellTiter-Blue Viability Assay (Promega) and a microplate reader. The percentage of cell viability was expressed relative to that of untreated control in each group.

Annexin V assay

APC Annexin V kit (Biolegend, Cat# 640920) was used following the manufacturer's instructions. In general, cells were dissociated with 0.02% EDTA solution, washed with 1% BSA in PBS. Cells were then stained with 5 μL APC-Annexin V in 100 μL Annexin V binding buffer and Sytox Blue (Biolegend, 50 nM) on ice and then samples were run on an LSR Fortessa X-20 (BD) and analyzed using FlowJo software (TreeStar).

Sphere formation assay

Cancer cells were seeded as single-cell suspension at 200-2000 cells/well in 24-well ultra-low

attachment plates (Sigma Aldrich). The sphere formation medium was serum-free DMEM or RPMI 1640 supplemented with 5 μg/ml insulin (Sigma Aldrich), and 20 ng/ml human recombinant EGF (Thermo Fisher Scientific), 10 ng/ml FGF-basic (Sigma Aldrich), and 2% B27 (Invitrogen). At the end point, the spheres were photographed and the number of spheres (>50 μm) was counted under microscope.

Real time PCR

The RNA was reverse transcribed into cDNA using High-Capacity cDNA Reverse Transcription Kit (Thermo Fisher Scientific). Real-time PCR was performed using iTaq™ Universal SYBR® Green Supermix (Bio-Rad). Relative mRNA expression of target genes was determined using the standard curve method, and then normalized to *GAPDH* mRNA as internal control. The primers of target genes for the real-time PCR are listed in Supplemental Table 5.

Cytokine array

A cytokine array (Raybiotech, Cat# AAH-CYT-5-4) was utilized according to the manufacturer's instructions. Integrated dot intensity was examined using Image J.

ELISA

Cells were seeded at 2×10^5 cells in duplicates or triplicates in 6-well tissue culture plates and allowed to adhere overnight. Cells were then grown in serum-free medium for 24 hours. The cell supernatants were collected by medium centrifugation and filtration through 0.45 μm filter. OPN ELISAs were processed in accordance with the manufacturer's instructions (R&D, Cat# DOST00). CAM1 and CAM2 have two biological replicates, while all other samples have 3 biological replicates. TGFβ1 ELISA was processed in accordance with the manufacturer's instructions of TGFβ1 ELISA kit (R&D, Cat# DB100B) and sample activation kit (R&D, Cat# DY010).

OPN shRNA knockdown

Two shRNAs against *OPN* (*SPP1)* were purchased from Sigma Aldrich (TRCN0000004875 and TRCN0000342616). For the generation of lentiviral particles, 293T cells were transfected by a cocktail of 1.5 μg sh*OPN* or non-targeting control constructs, packaging vectors (0.5 μg of *VSVG* and 2 μg of *Δ8.2*) and Lipofectamine 2000 (Thermo Fisher Scientific). The lentiviral supernatants were harvested at 48 and 72 hours post-transfection using 0.45 μm filter, and added to LP9 cells with 5 μg/ml Polybrene. The lentivirus infected LP9 cells were then selected with puromycin (1 mg/ml) for 5 days until control cells without infection were all dead.

Western blotting

Cells were lysed in RIPA buffer with the addition of protease or phosphatase inhibitors and cleared by centrifugation (12,000 rcf for 15 minutes at 4°C). Proteins were separated by gel electrophoresis and 20–50 μg of protein was subjected to reducing SDS/PAGE using standard methods (6). Blots were probed with the primary antibodies (1:1000) overnight at 4°C; or anti-GAPDH antibody (1:2000) as loading control. After washing, blots were incubated with anti-rabbit or anti-mouse IgG HRP-linked secondary antibodies (Cell Signaling Technologies, 1:5000) at room temperature for 1 hour. Immunoblots were developed with SuperSignal West Dura Extended Duration Substrate or SuperSignal West Femto Maximum Sensitivity Substrate (Thermo Fisher Scientific) and visualized with ChemiDoc XRS. Imaging system equipped with Image Lab Software (Bio-Rad).

Aldefluor assay

For the detection of ALDH1 activity, Aldefluor assay kit (STEMCELL Technologies, Cat# 01700) was used according to the manufacturer's instructions. Briefly, dissociated cancer cells from co-culture or xenografts were resuspended in Aldefluor assay buffer containing ALDH1 substrate at 1.5 mM, and incubated for 40 minutes at 37°C. For each sample, half of cell samples was treated

with 50 mM diethylaminobenzaldehyde (DEAB) to define negative gates, the other half was used as test tube in the absence of DEAB.

For analysis on in vivo xenografts, subcutaneous tumors were carefully dissected. Tumors were digested in 20 μg/ml Liberase and 400 μg/ml DNase I in RPMI 1640 for 30 minutes at 37°C with rotation. After tissue digestion, loosely attached tissues were minced into 2-5 mm pieces using scissors, mashed with the plunger of 5 ml syringe and filtered through a cell strainer to get rid of tissue clumps. The filtered mixture was then added with 30% Percoll gradient in RPMI 1640 and centrifuged with no brakes for 20 minutes. The cell pellets were then resuspended in full RPMI 1640 medium to generate single cell suspensions. After processed with Aldefluor assay procedures as mentioned above, cell samples were stained with fluorescent labeled antibodies in Aldefluor assay buffer for 20 minutes at 4°C. After antibody labeling, cells were added with Sytox Blue and analyzed for ALDH1 percentage on an LSR Fortessa X-20 (BD) and analyzed using FlowJo software (TreeStar). The staining antibodies included Mouse Anti-EpCAM Antibody eFluor 660 (Thermo Fisher Scientific, 1:50), Mouse Anti-H-2Kd PE Antibody (BD, 1:50). Single color controls were used for compensation. All analysis was performed with FlowJo, and gating strategy was shown in Supplemental Figure 5J.

Flow cytometry of cell surface makers

For cell surface marker analysis, 1-5 x 10^6 cells were dissociated with 0.02% EDTA in PBS, and washed and resuspended in PBS containing 1% BSA. Cells were then stained with primary antibodies (CD44, Bioxcell, 1:50; Integrin αV, Biolegend, 1:50; Integrin β1, DSHB, 1:50) for 20 minutes on ice. After brief centrifugation and washes for two times with PBS containing 1% BSA, cells were incubated with Alexa Fluor-conjugated secondary antibodies (Thermo Fisher Scientific, 1:200) for 20 minutes on ice. After brief centrifugation and washes, cells were added with Sytox

Blue (Biolegend) and immediately analyzed. Samples were run on an LSR Fortessa X-20 (BD) and analyzed using FlowJo software (TreeStar).

EFLUXX-ID® Green multidrug resistance assay

The functions of the multidrug resistance proteins MDR1, MRP and BCRP were analyzed by eFluxx-ID Green Multidrug Resistance Assay Kit (ENZ-51029-K100, Enzo Lifesciences, Farmingdale, NY) according to the manufacturer's instructions as previously reported (7). Briefly, after treatment, 2 x 10^5 cells were collected, washed with PBS and resuspended in complete growth medium without Phenol Red. Cells were then incubated with or without MDR inhibitors (verapamil for P-gp, MK-571 for MRP1, and novobiocin for BCRP, and DMSO for untreated control) for 5 min at 37 °C, and incubated with the eFluxx-IDH Green dye for 30 min at 37 °C. Propidium iodide (PI) was added to the cells during the last 5 min of incubation for live cell detection. After data acquisition on LSR Fortessa X-20 (BD), the results were analyzed with FlowJo software. To quantify the transporter activity, the multidrug resistance factor (MAF) value was calculated using the following formula for each respective inhibitor: MAF = 100 x (MFI with inhibitor - MFI control)/MFI with inhibitor, where MFI = mean fluorescence intensity. For each inhibitor, MAF values from three samples were used to calculate the mean MAF value.

3D organoid culture

Live $EpCAM^+$ cancer cells were FACS (fluorescence-activated cell sorting) sorted from cryopreserved ovarian cancer patient specimen and subjected to 3D hydrogel encapsulation. For 3D encapsulation, sorted $EpCAM^+$ ovarian cancer cells were counted, pelleted for 5 minutes at 600 x g, and homogeneously resuspended in ice-cold Cultrex (Trevigen) for a final cell concentration of 1000 cells/µL. For each hydrogel replicate, 20 µL of cell/Cultrex solution was pipetted into a single well of a 24-well plate containing a custom cylindrical silicone mold (5 mm

diameter x 0.8 mm height) bonded to a circular 12 mm diameter glass cover slip, as previously reported (8). Hydrogel solutions were then incubated for 20 minutes at 37 °C to allow for Cultrex gelation. Following gelation, 700 µL of complete CAM CM or complete control medium was added to each well. Initial medium was supplemented with 2.5 µM GSK-3 inhibitor CHIR99021 (Cayman Chemical) and 10 µM ROCK inhibitor Y27632 (STEMCELL Technologies) for the first three days in culture. Cell cultures were incubated at 37 °C and allowed to grow for 27 days. Culture medium was replaced every 3 days.

Paired primary CAM at 80% confluence was cultured for 72 hours, and the CAM CM was collected and filtered through 0.45 µm filter. This CAM CM was not concentrated. The filtered CAM CM was then mixed at 1:1 ratio with organoid formation medium to generate complete CAM CM. Complete control medium was generated from unconditioned medium containing 40% Ham's F-12, 40% Medium M199, 20% FBS, mixed with organoid formation medium at 1:1 ratio.

Organoid formation medium consisted of complete WENR medium (Advanced DMEM/F-12 (Gibco) supplemented with 50% Wnt3a, R-spondin-1, and Noggin conditioned medium (L-WRN cells; ATCC) with 1X GlutaMAX (Gibco), 1 mM HEPES (Thermo Fisher Scientific), 50 ng/ml human EGF (Peprotech), 10 ng/ml human FGF2 (Peprotech), 10 ng/ml human FGF10 (Peprotech), 10 mM Nicotinamide (Sigma), 1 mM N-Acetylcysteine (Sigma), 1X B27 Supplement, minus vitamin A (Gibco), 0.5 µM A83-01 (Sigma Aldrich), 1X Penicillin-Streptomycin-Glutamine (Thermo Fisher Scientific), 10 nM Gastrin (Sigma Aldrich), 10 µM SB-202190 (Peprotech), 100 µg/ml Normocin (Invivogen)).

Immunostaining of 3D hydrogel organoids

3D cultures in Cultrex hydrogels were fixed with 4% paraformaldehyde and 0.1% glutaraldehyde in PBS for 30 minutes at room temperature. Samples were then washed with 200 mM glycine in

PBS for 1 minute and again for 15 minutes to quench any remaining glutaraldehyde, followed by two more washes in PBS. Samples were permeabilized with 0.1% Triton X-100 in PBS (PBST) for 1 hour and blocked with 10% goat serum in PBST for 4 hours, both at room temperature. Samples were incubated with primary antibody (ALDH1A1; Santa Cruz, 1:50) solution overnight at 4 °C. The following day, samples were washed three times and incubated at 4°C overnight with secondary antibody (anti-Mouse IgG Alexa Fluor 546; Invitrogen, 1:500). The following day, samples were washed three times with PBST. Next, 4′,6-diamidino-2-phenylindole (DAPI; Sigma Aldrich) and Alexa Fluor 647 phalloidin (F-actin stain; diluted in methanol; Invitrogen) were diluted in PBST for a final concentration of 2.5 μg/ml and 165 nM, respectively. Samples were incubated with DAPI and phalloidin for 1 hour at room temperature and subsequently washed three times. Samples were imaged using a Leica SPE confocal microscope.

The 3D volume image, covering a volume of 91x91x36.5 μm (voxel size: 0.089x0.089x0.5 μm), was collected with a Nikon Eclipse Ti2-E inverted confocal microscope using a C2 mirror scanner, modified to include a coherent anti-Stokes Raman scattering (CARS) excitation/detection channel for lipid-specific imaging. The 3D rendering was created in NIS Elements.

Immunostaining of paraffin embedded organoids

3D cultures in Cultrex hydrogels were fixed with 4% paraformaldehyde and 0.1% glutaraldehyde in PBS for 24 hours at 4°C. Following fixation, samples were washed with 200 mM glycine in PBS for 1 minute and again for 15 minutes to quench any remaining glutaraldehyde, followed by two more washes in PBS for 15 minutes each. Hydrogels were removed from the silicone molds, transferred to a histology cassette, and submerged in 70% ethanol. Samples were provided to the Stanford Human Pathology/Histology Service Center for paraffin embedding, sectioning, and H&E staining. H&E stained slides were imaged using a Leica SPE microscope. For deparaffinizing

of unstained sections, slides were placed in xylene, gradient ethanol, and then DI water. For antigen retrieval, slides were submerged in sodium citrate buffer (10 mM sodium citrate, 0.05% Tween-20, pH 6.0) and incubated in a steamer (IHC World) for 45 minutes. After allowing slides to cool, samples were washed three times with PBS, permeabilized with 0.2% Triton X-100 in PBS for 15 minutes, and blocked with 10% goat serum in 0.2% Triton X-100 in PBS for 2 hours, all at room temperature. Primary antibodies (CD44, Bioxcell, 1:50; Pan-cytokeratin, Abcam, 1:100; Cytokeratin 8, DSHB, 1:25; EpCAM, Abcam, 1:50) diluted at 1:100 were incubated with samples overnight at 4°C. Samples were then washed with PBST five times for 5 minutes each at room temperature. Secondary antibodies (anti-Rabbit IgG Alexa Fluor 488, anti-Rat IgG Alexa Fluor 647, anti-Rat IgG Alexa Fluor 546, anti-Rabbit IgG Alexa Fluor 647, Thermo Fisher Scientific, 1:500) and DAPI (Sigma Aldrich, 2.5 μg/ml) were diluted in PBST and incubated with samples for 2 hours at room temperature. Samples were again washed with PBST five times and mounted using ProLong Gold Antifade Reagent (Cell Signaling Technologies). Samples were imaged using a Leica SPE confocal microscope.

Immunostaining of OPN in cell cultures

Cells were cultured into 8-well chamber slide (Thermo Fisher Scientific), and fixed in 4% paraformaldehyde for 20 minutes. Cells were permeabilized with 0.2% Tween-20 in PBS, blocked in serum-free protein block (Dako) for 10 minutes at room temperature, and then stained in primary antibody (Rabbit Anti-osteopontin Antibody, Abcam, 1:100) solution at room temperature for 1 hour. After washing, secondary antibodies conjugated with Alexa Fluor Dyes (Anti-rabbit Alexa Fluor 555 Secondary Antibody, 1:400) were added for 30 minutes at room temperature. DAPI (Sigma Aldrich) was used for nuclear counterstaining at 0.1 μg/ml. Fluorescence images were collected with a Nikon Eclipse Ti2-E inverted confocal microscope equipped with a C2 mirror

scanner. DAPI (nuclei) were excited at 405 nm and detected in the range 440-475 nm. Alexa Fluor 555 (OPN) was excited at 561 nm and detected in the range 575-610 nm. Stitched 3D images (4x4 stacks) covering a total volume of 408x408x20 μm (3789x3789x5 pixels) were randomly collected with a voxel size of (0.11x0.11x4 μm). Images were pre-processed and analyzed using ImageJ. Briefly, following Gaussian blurring and max projection, the cell nuclei were identified by Li thresholding. Connecting nuclei were separated by the Ellipse Split plug-in, using a standard watershed routine. Nuclei were used as seeds for Voronoi segmentation of the cells. The mean fluorescence intensity was calculated for each cell. Forty-three LP9 cells and 186 OC8 cells were evaluated.

Immunostaining of human specimens

Formalin-fixed, paraffin-embedded samples were sectioned to 4-5 μm thickness, and the slides were deparaffinized in xylene and rehydrated through graded ethanol solutions. Antigen retrieval was conducted in pressure cooker for 10 minutes using sodium citrate buffer (10 mM sodium citrate, 0.05% Tween-20, pH 6.0). Slides were then blocked with serum-free protein block (Dako) for 10 minutes at room temperature to reduce non-specific staining. After blocking, samples were performed staining at 4°C overnight using primary antibodies (Rabbit Anti-osteopontin Antibody, Abcam, 1:100; Mouse anti-calretinin Antibody, Invitrogen, 1:50) diluted in PBS with 1% BSA and 0.05% Tween-20. On the next day, slides were incubated with Alexa Fluor-conjugated anti-mouse and anti-rabbit secondary antibodies (Thermo Fisher Scientific, 1:500) diluted in PBS with 1% BSA and 0.05% Tween-20 for 1 hour at room temperature. 0.2% Sudan Black B solution in 70% ethanol was then added to the slides through syringe filter for 10 minutes to quench background fluorescence. DAPI (Sigma Aldrich) was used for nuclear counterstaining at 0.1 μg/ml on the slides and images were taken under Leica SPE microscope.

For total ascites cells, single cell suspension was suspended in 100μL PBS and were deposited by cytospin onto glass slides. Cells were then fixed in 10% formalin for 20 mins, and blocked (30 min with normal serum). Cells were permeabilized with 0.2% Tween-20 in PBS, blocked in serum-free protein block (Dako) for 10 minutes at room temperature, and then stained in primary antibody (Rabbit Anti-osteopontin Antibody, Abcam, 1:100; Mouse Anti-calretinin Antibody, Invitrogen, 1:50) solution at room temperature for 1 hour. After washing, anti-rabbit and anti-mouse secondary antibodies conjugated with Alexa Fluor Dyes were added for 30 minutes at room temperature. DAPI (Sigma Aldrich) was used for nuclear counterstaining at 0.1 μg/ml and images were taken under Leica SPE microscope.

Immunostaining of mouse xenografts

Staining was performed on formalin-fixed, paraffin-embedded xenograft sections using the protocol described above for human omental specimens. Generally, sections were incubated with primary antibody against cleaved caspase-3 (Cell Signaling Technologies, 1:100), γ-H2AX (Cell Signaling Technologies, 1：500) or cisplatin-DNA adduct (Abcam, 1:100) at 4°C overnight, and incubated with Alexa Fluor-conjugated Anti-rabbit or Anti-rat Antibody (Thermo Fisher Scientific, 1:500) for 1 hour at room temperature. DAPI (Sigma Aldrich) was used for nuclear counterstaining. at 0.1 μg/ml on the slides and images were taken under the Leica SPE microscope.

Bioinformatics

GSE84829 was obtained from the Gene Expression Omnibus (GEO) and analyzed for DEGs in HPMCs and CAMs. GSE30587 was obtained from the GEO database and analyzed for *OPN* correlation with *Calretinin* on human omental metastatic tissues. For GSE9891 from the GEO database, serous-type tumor samples with primary site as “OV” and arrayed site as “PE” were

analyzed for peritoneal site gene expression correlations. Correlation analysis of gene expression and overall survival was performed only on "dead (D)" patients within the criteria.

References

1. Wang W, Kryczek I, Dostal L, Lin H, Tan L, Zhao L, et al. Effector T Cells Abrogate Stroma-Mediated Chemoresistance in Ovarian Cancer. *Cell.* 2016;165(5):1092-105.
2. Natarajan S, Foreman KM, Soriano MI, Rossen NS, Shehade H, Fregoso DR, et al. Collagen Remodeling in the Hypoxic Tumor-Mesothelial Niche Promotes Ovarian Cancer Metastasis. *Cancer Res.* 2019;79(9):2271-84.
3. Wu YJ, Parker LM, Binder NE, Beckett MA, Sinard JH, Griffiths CT, et al. The mesothelial keratins: a new family of cytoskeletal proteins identified in cultured mesothelial cells and nonkeratinizing epithelia. *Cell.* 1982;31(3 Pt 2):693-703.
4. Li J, Yousefi K, Ding W, Singh J, and Shehadeh LA. Osteopontin RNA aptamer can prevent and reverse pressure overload-induced heart failure. *Cardiovasc Res.* 2017;113(6):633-43.
5. Halder SK, Beauchamp RD, and Datta PK. A specific inhibitor of TGF-beta receptor kinase, SB-431542, as a potent antitumor agent for human cancers. *Neoplasia.* 2005;7(5):509-21.
6. Rankin EB, Fuh KC, Castellini L, Viswanathan K, Finger EC, Diep AN, et al. Direct regulation of GAS6/AXL signaling by HIF promotes renal metastasis through SRC and MET. *Proc Natl Acad Sci U S A.* 2014;111(37):13373-8.
7. Mo L, Pospichalova V, Huang Z, Murphy SK, Payne S, Wang F, et al. Ascites Increases Expression/Function of Multidrug Resistance Proteins in Ovarian Cancer Cells. *PLoS One.* 2015;10(7):e0131579.

8. Madl CM, LeSavage BL, Dewi RE, Dinh CB, Stowers RS, Khariton M, et al. Maintenance of neural progenitor cell stemness in 3D hydrogels requires matrix remodelling. *Nat Mater.* 2017;16(12):1233-42.

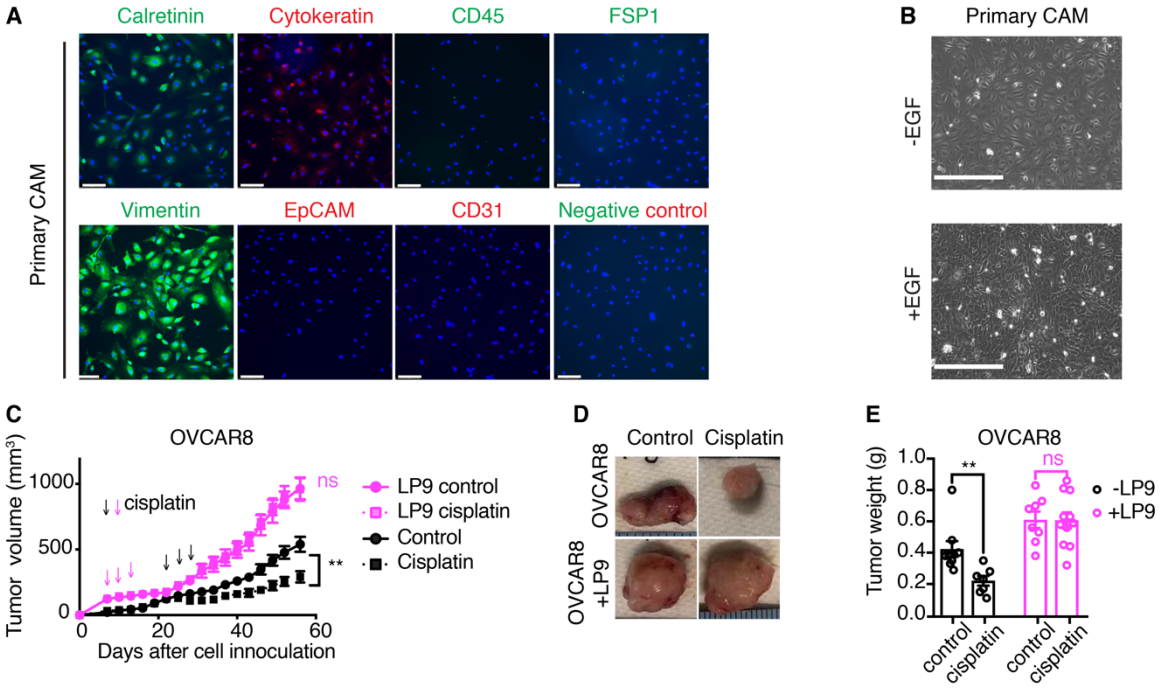

Supplemental Figure 1. Cancer associated mesothelial cells promote ovarian cancer cell cisplatin resistance.
(**A**) Immunofluorescence of cell type markers in primary mesothelial cells isolated from ovarian cancer patients. Nuclei were stained with DAPI (blue). Scale bars, 100 µm. (**B**) Morphology of primary isolated mesothelial cells in culture in the presence or absence of EGF. Scale bars, 400 µm. (**C-E**) Effect of LP9 co-injection on cisplatin resistance of OVCAR8 in vivo. OVCAR8 or OVCAR8 plus LP9 cells were injected subcutaneously into female immunodeficient mice and treated with or without cisplatin every 3 days for three cycles. Tumor growth curve is shown in C (n = 7-11 mice per group, mean ± SEM; **p<0.01, ns, not significant; two-tailed Student's t-test). Representative xenograft images are shown in D. Xenograft weights at the end point are shown in E (mean ± SEM; **p<0.01, ns, not significant; two-tailed Student's t-test).

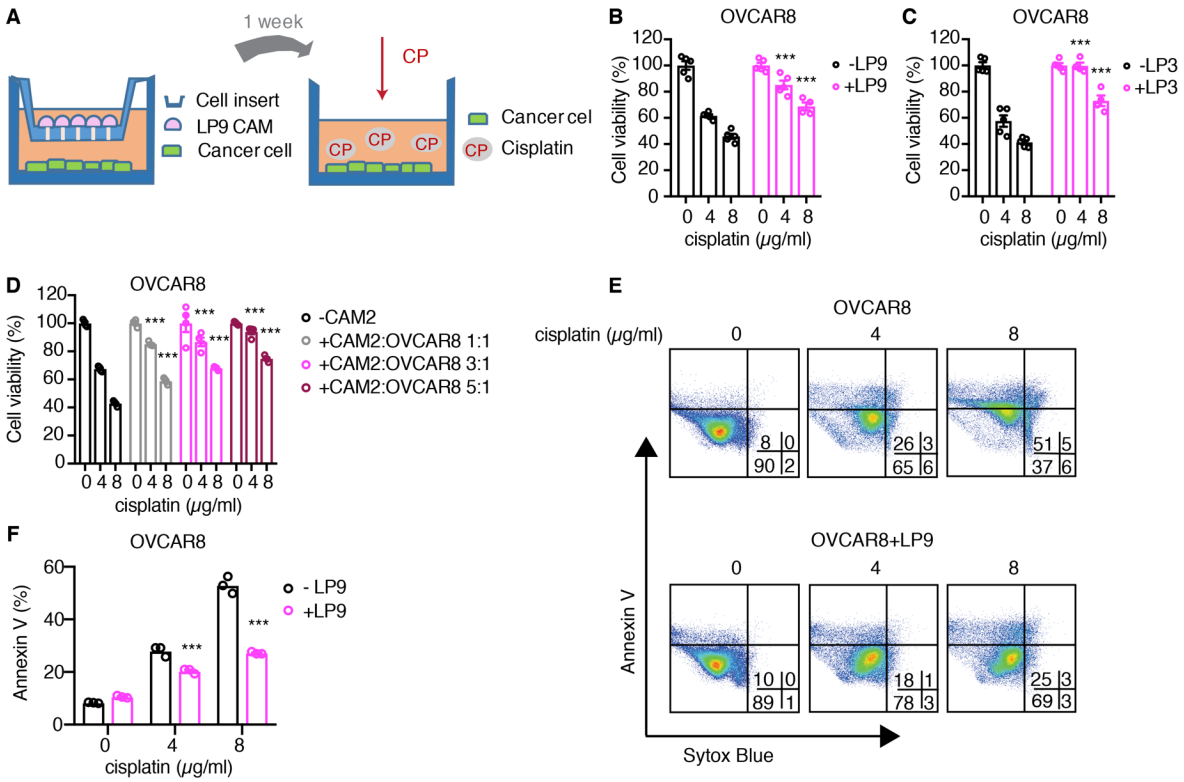

Supplemental Figure 2. Cancer associated mesothelial secreted factor(s) promote ovarian cancer cisplatin resistance.

(**A**) Schematic of the experimental approach showing the interaction between mesothelial cells and cancer cells in the indirect co-culture system. The 0.4 μm pore size insert allows mutual media exchange and avoids physical contact of two cell types. After co-incubation, chemotherapeutic drugs such as cisplatin was added only to the cancer cells, and the cancer cells were checked for phenotypic changes. (**B-C**) Effect of LP9 or LP3 co-culture on cisplatin sensitivity of OVCAR8. Cell viability is normalized to its untreated control (n=4-5; mean ± SEM; ***p<0.001 versus OVCAR8 monoculture; two-way ANOVA test). (**D**) CAM2 cells were co-cultured with OVCAR8 at ratios (1:1, 3;1, 5:1), and OVCAR8 cells were measured for cisplatin sensitivity after co-culture (n=3; mean ± SEM; ***p<0.001 versus OVCAR8 monoculture; two-way ANOVA test). (**E-F**) The percentage of Annexin V^+ apoptotic OVCAR8 cells with or without LP9 preconditioning. Representative image of Annexin V assay is shown in E, and quantification is shown in F (n=3; mean ± SEM; ***p<0.001 versus OVCAR8 monoculture; two-way ANOVA test).

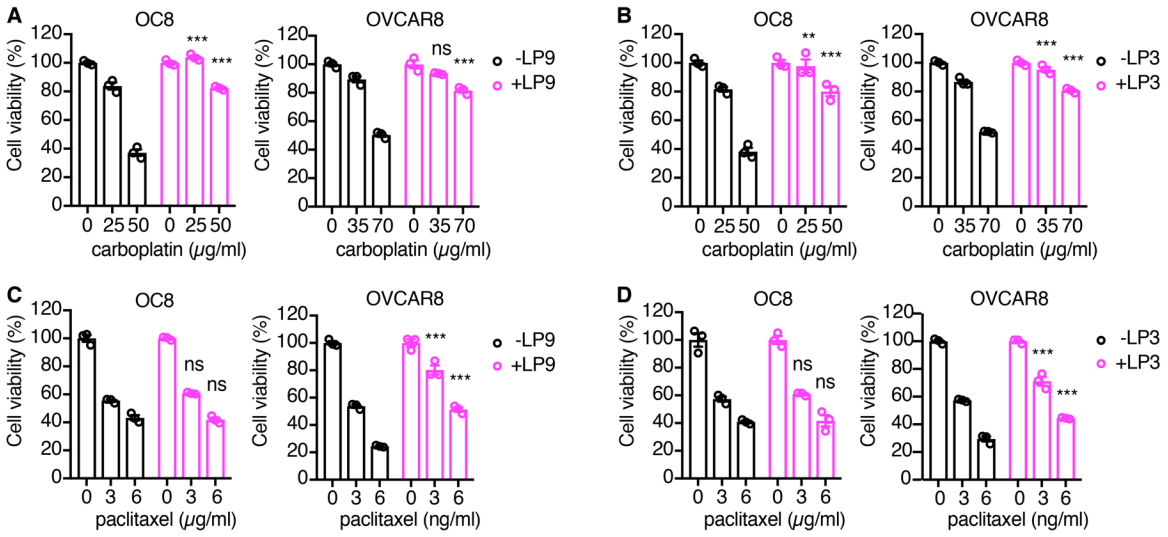

Supplemental Figure 3. Cancer associated mesothelial cells secreted factor(s) to promote ovarian cancer multidrug chemoresistance.

(**A-B**) Cell viability of OC8 and OVCAR8 cells treated with carboplatin after LP9 or LP3 co-culture (n=3). (**C-D**) Cell viability of OC8 and OVCAR8 treated with paclitaxel after LP9 or LP3 co-culture (n=3; mean ± SEM; ***p<0.001 versus OC8 or OVCAR8 monoculture, ns, not significant; two-way ANOVA test).

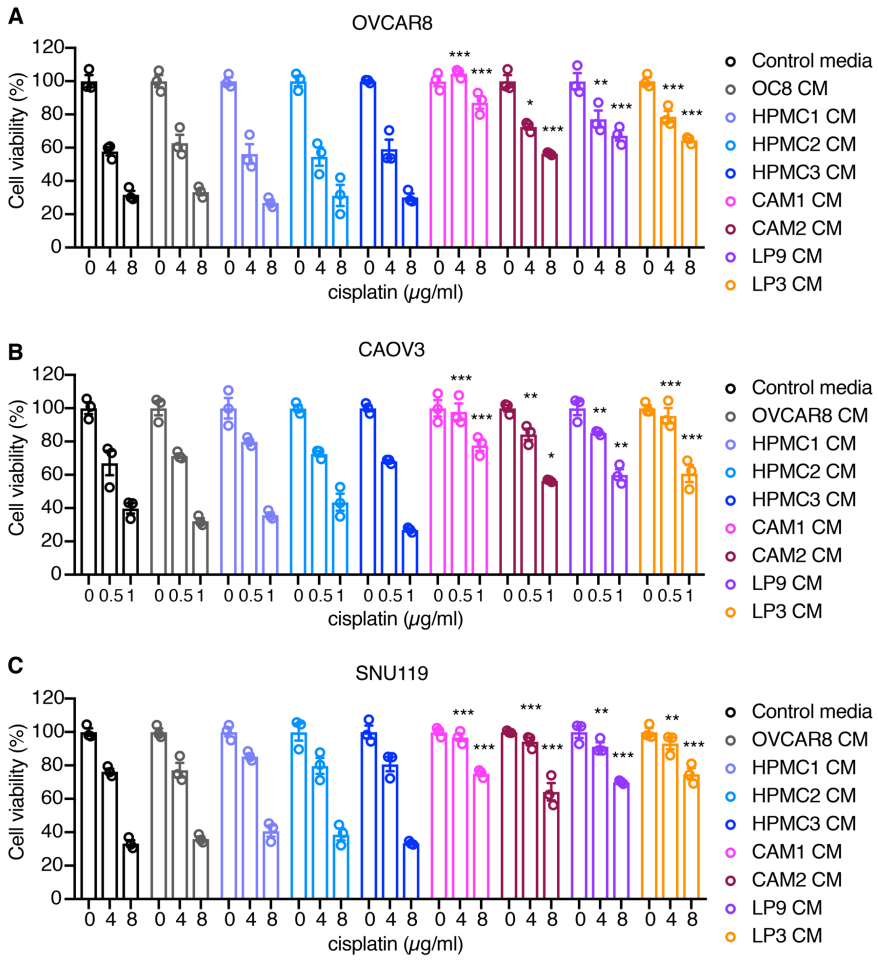

Supplemental Figure 4. Secreted factor(s) from cancer associated mesothelial cells, but not HPMCs, promote ovarian cancer chemoresistance.

(**A-C**) Effect of conditioned media (CM) from HPMCs or cancer associated mesothelial cells on the cisplatin sensitivity of OVCAR8, CAOV3 or SNU119 cells. Cell viability is normalized to its untreated control (n=3; mean ± SEM; *p<0.05, **p<0.01, ***p<0.001 versus control media; two-way ANOVA test).

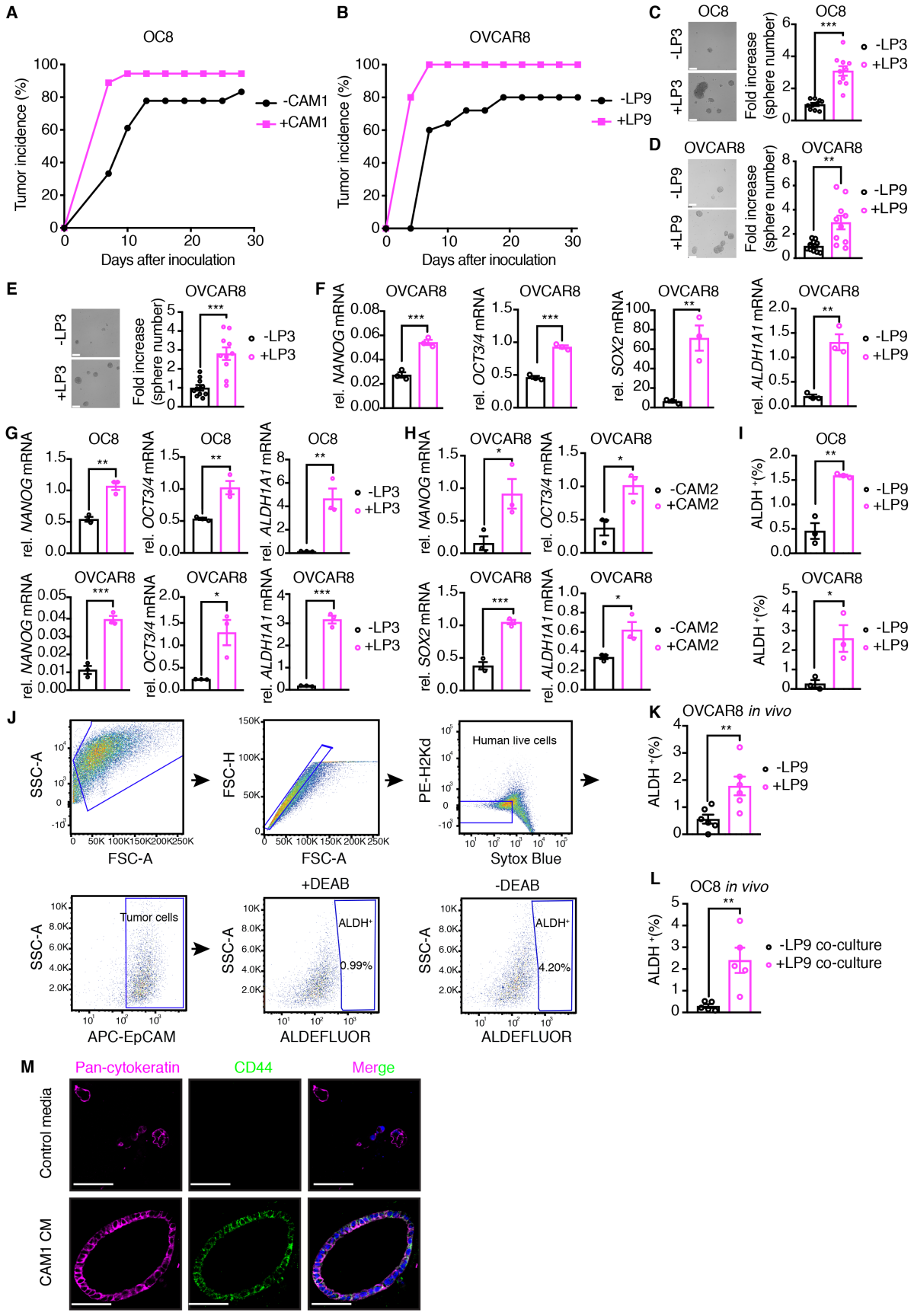
A
OC8
Tumor incidence (%)
Days after inoculation
-CAM1
+CAM1
B
OVCAR8
Tumor incidence (%)
Days after inoculation
-LP9
+LP9
C
OC8
-LP3
+LP3
Fold increase (sphere number)
D
OVCAR8
-LP9
+LP9
Fold increase (sphere number)
E
OVCAR8
-LP3
+LP3
Fold increase (sphere number)
F
OVCAR8
rel. NANOG mRNA
rel. OCT3/4 mRNA
rel. SOX2 mRNA
rel. ALDH1A1 mRNA
-LP9
+LP9
G
OC8
OVCAR8
rel. NANOG mRNA
rel. OCT3/4 mRNA
rel. ALDH1A1 mRNA
-LP3
+LP3
H
OVCAR8
rel. NANOG mRNA
rel. OCT3/4 mRNA
rel. SOX2 mRNA
rel. ALDH1A1 mRNA
-CAM2
+CAM2
I
OC8
OVCAR8
ALDH+(%)
-LP9
+LP9
J
SSC-A
FSC-A
FSC-H
PE-H2Kd
Sytox Blue
Human live cells
Tumor cells
APC-EpCAM
+DEAB
-DEAB
ALDH+
0.99%
4.20%
ALDEFLUOR
K
OVCAR8 in vivo
ALDH+(%)
-LP9
+LP9
L
OC8 in vivo
ALDH+(%)
-LP9 co-culture
+LP9 co-culture
M
Pan-cytokeratin
CD44
Merge
Control media
CAM1 CM

Supplemental Figure 5. Cancer associated mesothelial cells promote ovarian cancer stemness.
(**A**) Effect of CAM1 co-injection on tumor incidence of OC8 injected subcutaneously in immunodeficient mice. (**B**) Effect of LP9 co-injection on tumor incidence of OVCAR8 injected subcutaneously in immunodeficient mice. (**C**) Sphere formation assay of OC8 after LP3 co-culture. Representative sphere images are shown on the left. Quantification of sphere number are shown as fold increase on the right (n=10; mean ± SEM; ***p<0.001; two-tailed Student's t-test). Scale bar, 200 μm. (**D-E**) Sphere formation assay of OVCAR8 after LP9 or LP3 co-culture. Representative sphere images are shown on the left. Quantification of sphere number are shown as fold increase on the right (n=10; mean ± SEM; **p<0.01, ***p<0.001; two-tailed Student's t-test). Scale bar, 200 μm. (**F-H**) Relative mRNA quantification of stemness markers *NANOG, OCT3/4, SOX2* and *ALDH1A* in OVCAR8 with or without LP9 co-culture (F); OC8 and OVCAR8 cells with or without LP3 co-culture (G); OVCAR8 with or without CAM2 co-culture (H) as normalized to *GAPDH* mRNA in real-time PCR analysis (n=3; mean ± SEM; **p<0.01, ***p<0.001; two-tailed Student's t-test). (**I**) Aldefluor assay showing the proportion of $ALDH^+$ cells in OC8 and OVCAR8 with or without LP9 co-culture in vitro. (n=3; mean ± SEM; *p<0.05, **p<0.01; two-tailed Student's t-test). (**J-K**) Flow cytometry gating strategy of Aldefluor assay in live $EpCAM^+$ tumor cells in vivo (J). Cells were gated by SSC-A vs FSC-A to rule out debris and FSC-H vs FSC-A for singlets. The singlets were then gated by PE-H-2Kd for human cells and APC-EpCAM for epithelial cells. The DEAB added sample serves as a control for each tested sample in Aldefluor assay. K shows the frequency of $ALDH^+$ cells in $EpCAM^+$ population of OVCAR8 xenografts with or without LP9 co-injection in vivo measured by Aldefluor assay (n=6 mice per group, mean ± SEM; **p<0.01; two-tailed Student's t-test). (**L**) Aldefluor assay showing the frequency of $ALDH^+$ cells in $EpCAM^+$ population of OC8 xenografts with or without pretreatment of LP9 co-culture (n=5 mice per group, mean ± SEM; **p<0.01; two-tailed Student's t-test). (**M**) Immunofluorescent staining of pan-cytokeratin (magenta) and CD44 (green) in ovarian cancer organoids grown in CAM1 conditioned media (CM) or in control media. Scale bars, 50 μm.

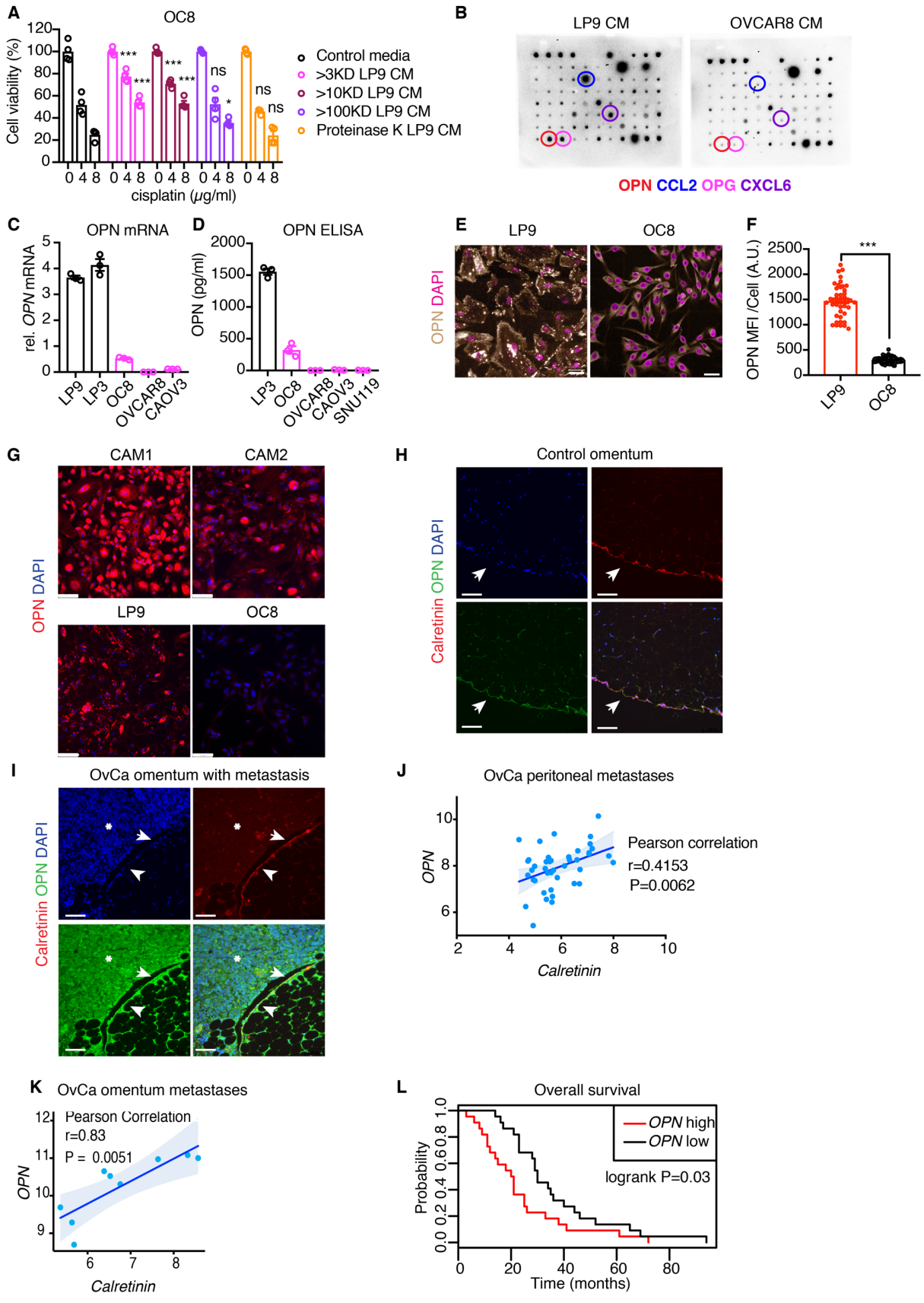
A
OC8
Cell viability (%)
cisplatin (μg/ml)
Control media
>3KD LP9 CM
>10KD LP9 CM
>100KD LP9 CM
Proteinase K LP9 CM
B
LP9 CM
OVCAR8 CM
OPN CCL2 OPG CXCL6
C
OPN mRNA
rel. OPN mRNA
LP9
LP3
OC8
OVCAR8
CAOV3
D
OPN ELISA
OPN (pg/ml)
LP3
OC8
OVCAR8
CAOV3
SNU119
E
LP9
OC8
OPN DAPI
F
OPN MFI /Cell (A.U.)
LP9
OC8
G
CAM1
CAM2
OPN DAPI
LP9
OC8
H
Control omentum
Calretinin OPN DAPI
I
OvCa omentum with metastasis
Calretinin OPN DAPI
J
OvCa peritoneal metastases
OPN
Calretinin
Pearson correlation
r=0.4153
P=0.0062
K
OvCa omentum metastases
Pearson Correlation
r=0.83
P = 0.0051
OPN
Calretinin
L
Overall survival
OPN high
OPN low
logrank P=0.03
Probability
Time (months)

Supplemental Figure 6. Cancer associated mesothelial cells secrete osteopontin.
(**A**) Effect of fractionated and proteinase K digested LP9 conditioned media (CM) on OC8 cell viability upon cisplatin treatment (n=3; mean ± SEM; *p<0.05, ***p<0.001 versus control media, ns, not significant; two-way ANOVA test). (**B**) Cytokine array in LP9 CM and OVCAR8 CM. Circles highlight cytokine of the highest fold change in each individual color. (**C**) Real time PCR analysis of relative mRNA expression of *OPN* in LP9 and LP3 CAMs, and ovarian cancer cells as normalized to GAPDH mRNA (n=3; mean ± SEM). (**D**) Quantification of OPN concentration in LP3 and ovarian cancer cell CM by ELISA. (n=3; mean ± SEM). (**E-F**) Representative images of OPN (gold) immunofluorescence in LP9 and OC8 are shown in E. DAPI was stained in magenta. Single cell quantification of mean OPN fluorescence intensity per cell is shown in F (n=43 in LP9, n=184 in OC8; mean ± SEM; ***p<0.001; two-tailed Student's t-test). Scale bars: 50 μm. (**G**) Representative immunofluorescent images of OPN (red) in CAM1, CAM2, LP9 and OC8. Scale bars, 100 μm. DAPI was stained in blue. (**H-I**) Immunofluorescence of OPN (green) and mesothelial cell marker calretinin (red) on control omentum from non-cancerous donors, or omentum with ovarian cancer (OvCa) metastasis from HGSOC patient. Arrows denote mesothelial cells or CAMs, asterisks mark metastasizing cancer cells in proximity. Nuclei were stained with DAPI (blue). Scale bars: 100 μm. (**J**) Correlation of *OPN* expression with *Calretinin* expression in human serous-type ovarian cancer peritoneal metastases (GSE9891, n=42; Pearson correlation). (**K**) Correlation of *OPN* expression with *Calretinin* expression in human serous ovarian cancer omental metastasis samples (GSE30587, n=9; Pearson correlation). (**L**) Kaplan-Meier curves of overall survival in ovarian cancer patients according to the median values of *OPN* expression in peritoneal metastases (GSE9891, n=44; log-rank test).

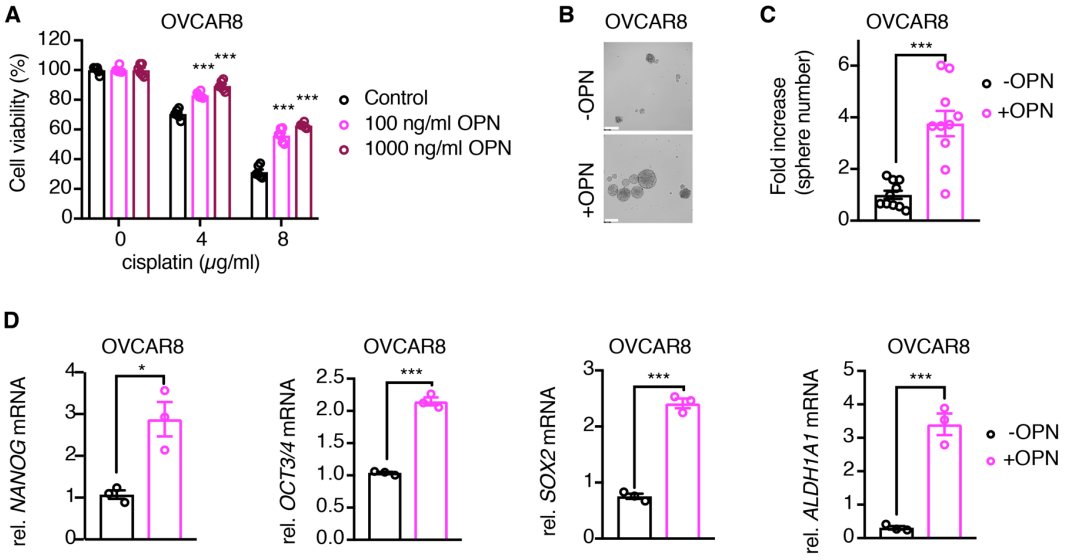

Supplemental Figure 7. Osteopontin promotes ovarian cancer chemoresistance and stemness. (**A**) Effect of exogenous OPN on cisplatin sensitivity of OVCAR8. Cell viability is normalized to its untreated control (n=3-5; mean ± SEM; ***p<0.001 versus untreated control; two-way ANOVA test). (**B-C**) Sphere formation assay of OVCAR8 after OPN exposure. Representative sphere images and quantification of sphere number fold increase are shown (n=10; mean ± SEM; ***p<0.001; two-tailed Student's t-test). Scale bar, 200 μm. (**D**) Real time PCR analysis showing relative mRNA expression of stemness markers *NANOG, OCT3/4, SOX2 and ALDH1A1* in OVCAR8 after OPN exposure, as normalized to *GAPDH* mRNA (n=3; mean ± SEM; *p<0.05, ***p<0.001; two-tailed Student's t-test).

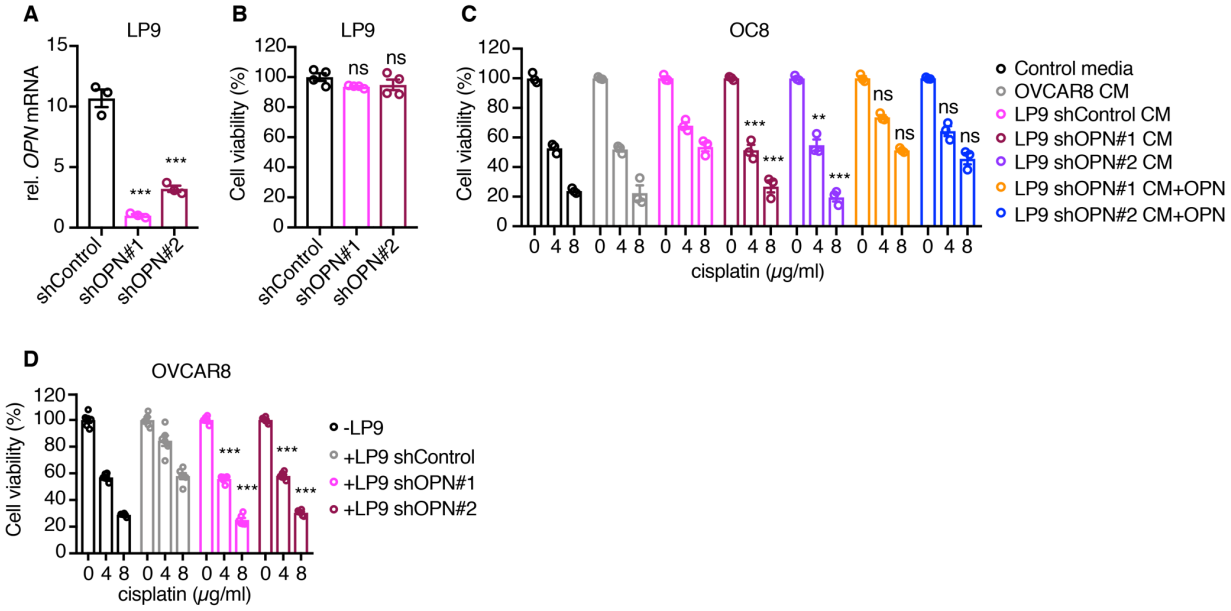

Supplemental Figure 8. Genetic inhibition of osteopontin reduces cancer associated mesothelial cell mediated ovarian cancer cisplatin resistance.

(**A**) Relative mRNA quantification of *OPN* expression in LP9 shControl and LP9 shOPN normalized to *GAPDH* mRNA as determined by real-time PCR (n=3; mean ± SEM; ***p<0.001 versus LP9 shControl; one-way ANOVA). (**B**) Cell viability of LP9 shOPN as normalized to shControl LP9 cell viability. (n=4; mean ± SEM; ns, not significant, versus LP9 shControl; one-way ANOVA test). (**C**) OC8 cells were exposed to LP9 shControl conditioned media (CM), LP9 shOPN CM or LP9 shOPN CM added with exogenous OPN, and tested for cell sensitivity to cisplatin. Cell viability of each group is normalized to its untreated control (n=3; mean ± SEM; **p<0.01, ***p<0.001 versus LP9 shControl CM, ns, not significant; two-way ANOVA test). (**D**) Cell viability of OVCAR8 cells treated with cisplatin after co-culture with LP9 shControl or LP9 shOPN. Cell viability is normalized to its untreated control (n=6; mean ± SEM; ***p<0.001 versus LP9 shControl; two-way ANOVA test).

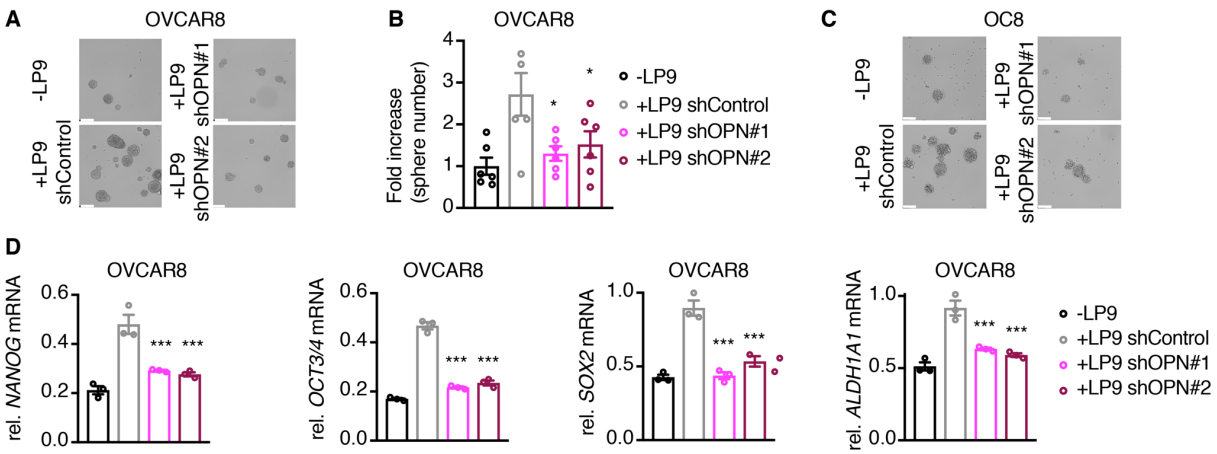

Supplemental Figure 9. Genetic inhibition of osteopontin reduces cancer associated mesothelial cell mediated ovarian cancer stemness.

(**A-B**) Sphere formation assay of OVCAR8 after co-culture with LP9 shControl or LP9 shOPN. Representative sphere images and quantification of sphere number fold increase are shown (n=6; mean ± SEM; *p<0.05 versus LP9 shControl; one-way ANOVA test). Scale bar, 200 μm. (**C**) Sphere formation assay of OC8 after co-culture with LP9 shControl or LP9 shOPN. Representative sphere images of sphere number fold increase are shown. Scale bar, 200 μm. (**D**) Real time PCR analysis showing relative mRNA expression of stemness markers *NANOG, OCT3/4, SOX2 and ALDH1A1* in OVCAR8 with LP9 shControl or LP9 shOPN co-culture, as normalized to *GAPDH* mRNA (n=3; mean ± SEM; ***p<0.001 versus LP9 shControl; one-way ANOVA test).

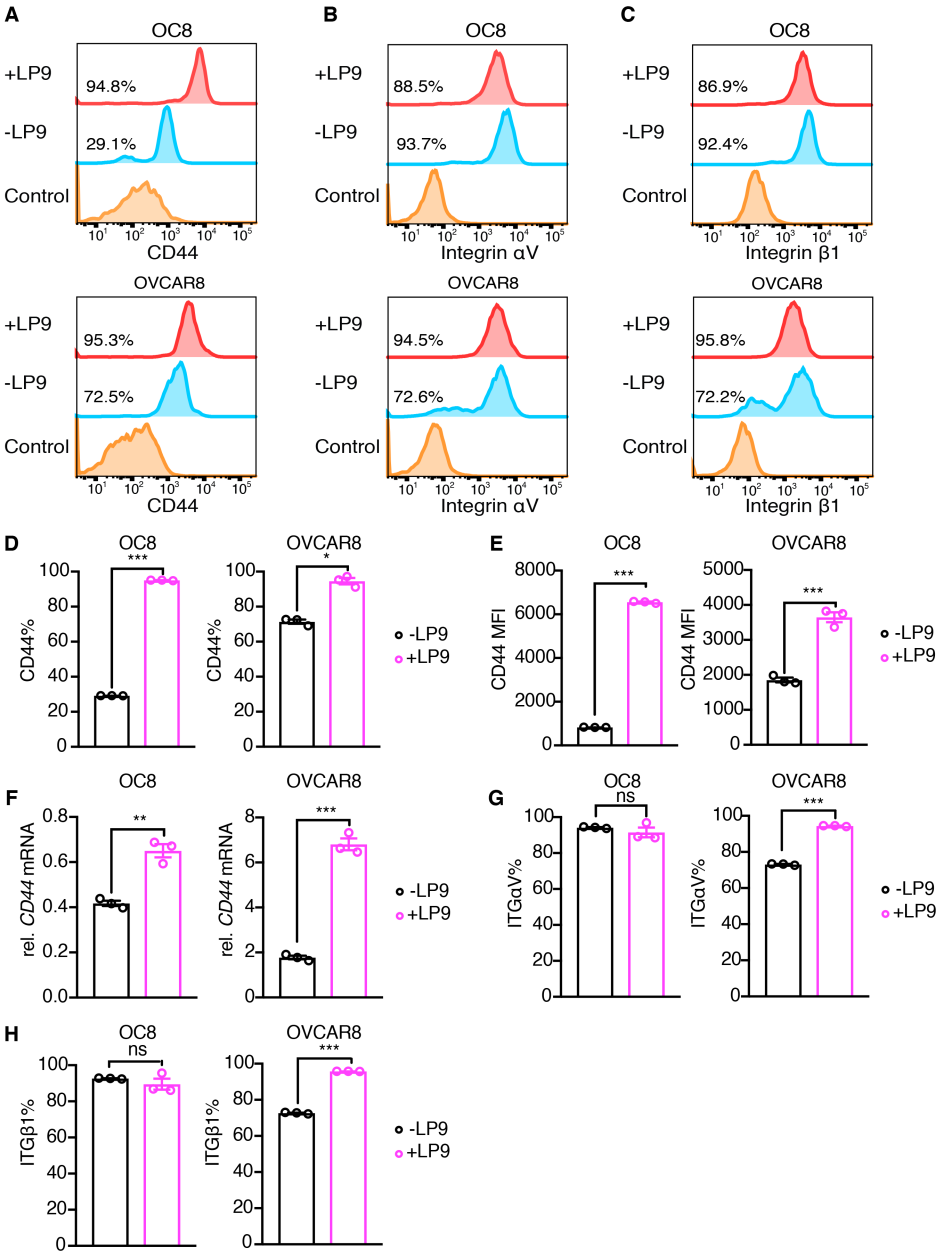

Supplemental Figure 10. CD44 and integrin expression on ovarian cancer cells co-cultured with cancer associated mesothelial cells.

(**A**) Percentage of $CD44^+$ cell OC8 and OVCAR8 cells with or without LP9 co-culture determined by flow cytometry. (**B**) Percentage of integrin αV^+ OC8 and OVCAR8 cells with or without LP9 co-culture determined by flow cytometry. (**C**) Percentage of integrin $\beta 1^+$ OC8 and OVCAR8 cells with or without LP9 co-culture determined by flow cytometry. (**D-E**) Quantification of $CD44^+$ percentages and CD44 median fluorescence intensity (MFI) in OC8 and OVCAR8 cells with or without LP9 co-culture (n=3; mean ± SEM; *p<0.05, ***p<0.001; two-tailed Student's t-test). (**F**) Relative mRNA quantification of *CD44* in OC8 and OVCAR8 cells with or without LP9 co-culture as normalized to *GAPDH* mRNA by real-time PCR. (n=3; mean ± SEM; **p<0.01, ***p<0.001; two-tailed Student's t-test). (**G-H**) Percentage of integrin αV^+ and integrin $\beta 1^+$ OC8 and OVCAR8 cells with or without LP9 co-culture. (n=3; mean ± SEM; ***p<0.001, ns, not significant; two-tailed Student's t-test).

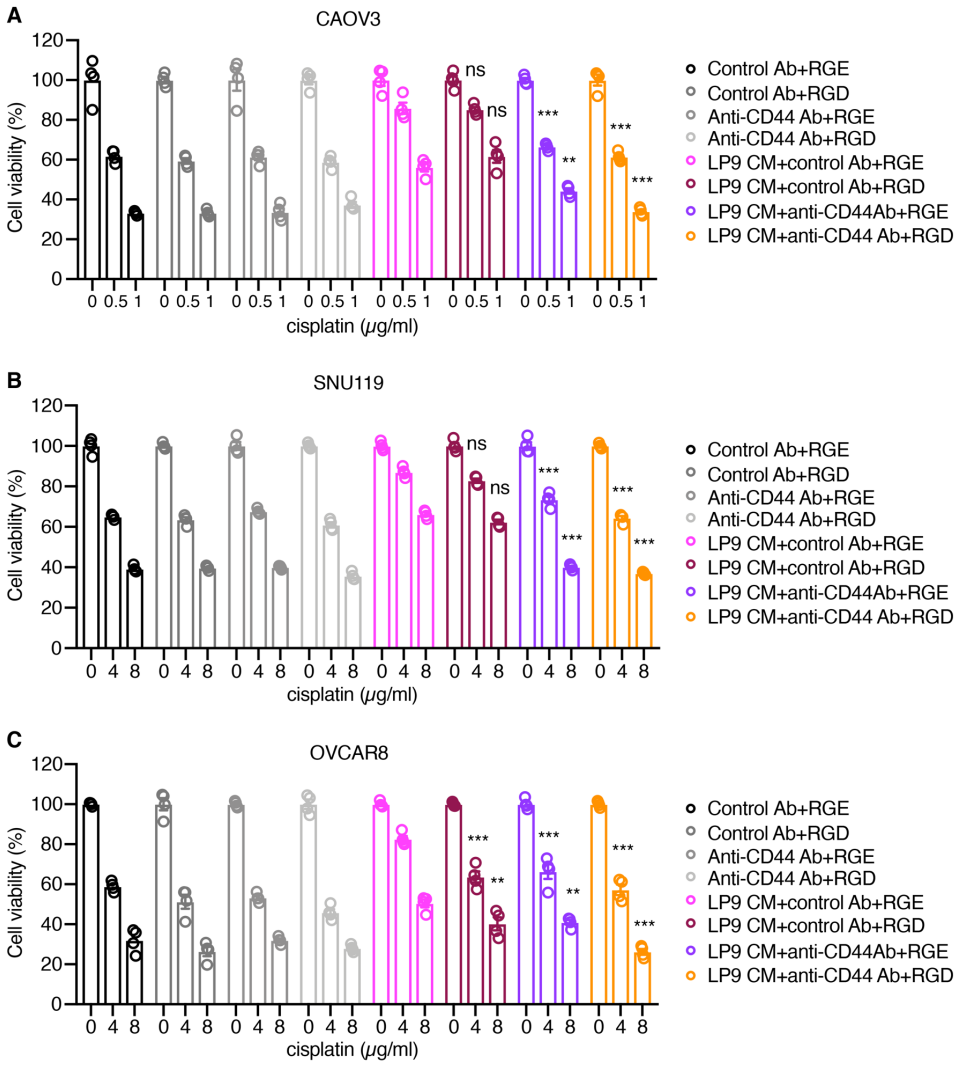

Supplemental Figure 11. CD44 receptor blockade reduces cancer associated mesothelial-induced ovarian cancer chemoresistance. (A-C) Effect of an anti-CD44 blocking antibody, integrin-blocking RGD peptide, or their combination on LP9 CM-mediated cisplatin resistance of CAOV3, SNU119 or OVCAR8 cells. RGE was used as control for RGD (n=4; mean ± SEM; **p<0.01, ***p<0.001 versus LP9 CM + control Ab + RGE; ns, not significant; two-way ANOVA test).

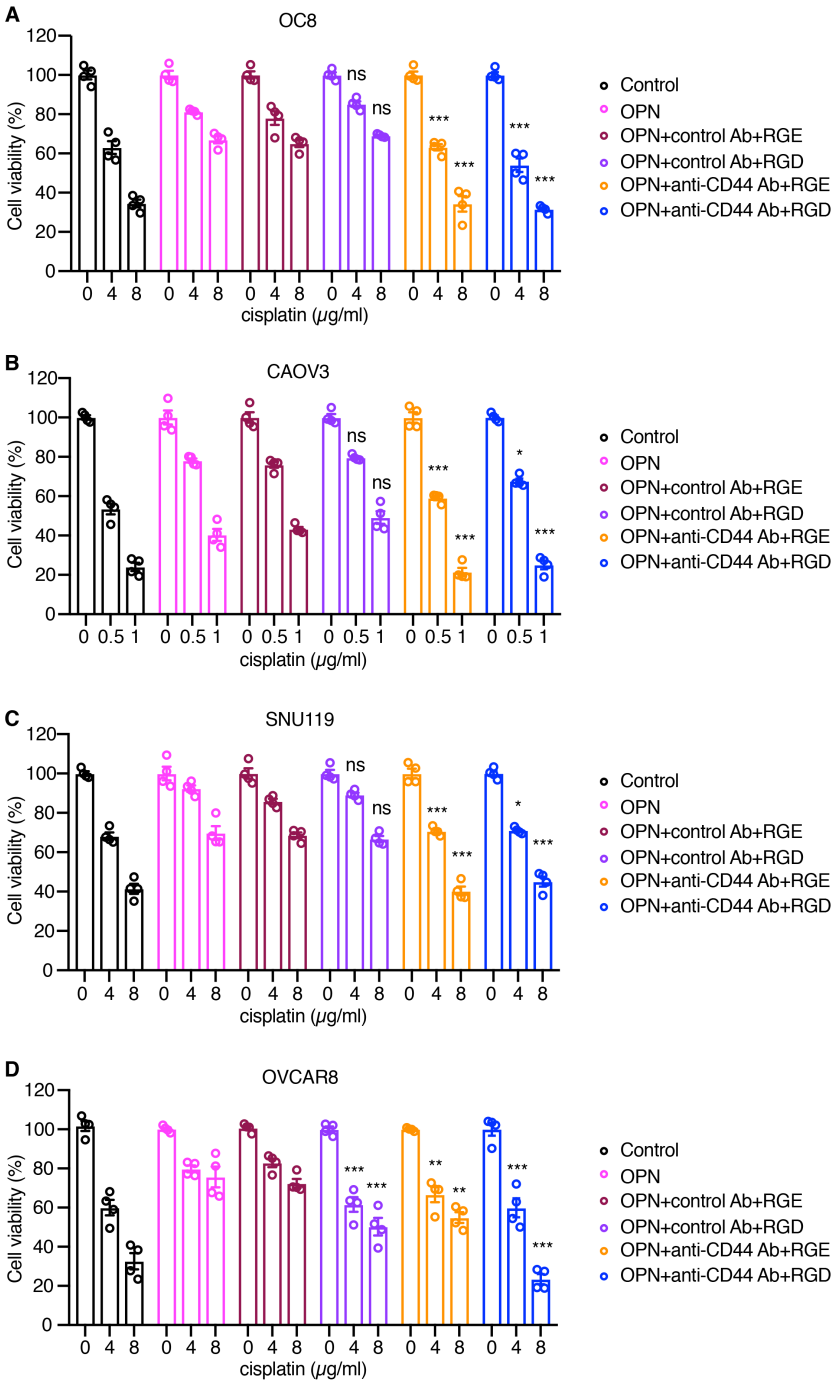

Supplemental Figure 12. CD44 receptor blockade reduces osteopontin-induced ovarian cancer chemoresistance. (**A-D**) Effect of an anti-CD44 blocking antibody, integrin-blocking RGD peptide, or their combination on OPN-mediated cisplatin resistance of OC8, CAOV3, SNU119 or OVCAR8 cells. RGE was used as control for RGD (n=4; mean ± SEM; *p<0.05, **p<0.01, ***p<0.001 versus OPN + control Ab + RGE; ns, not significant; two-way ANOVA test).

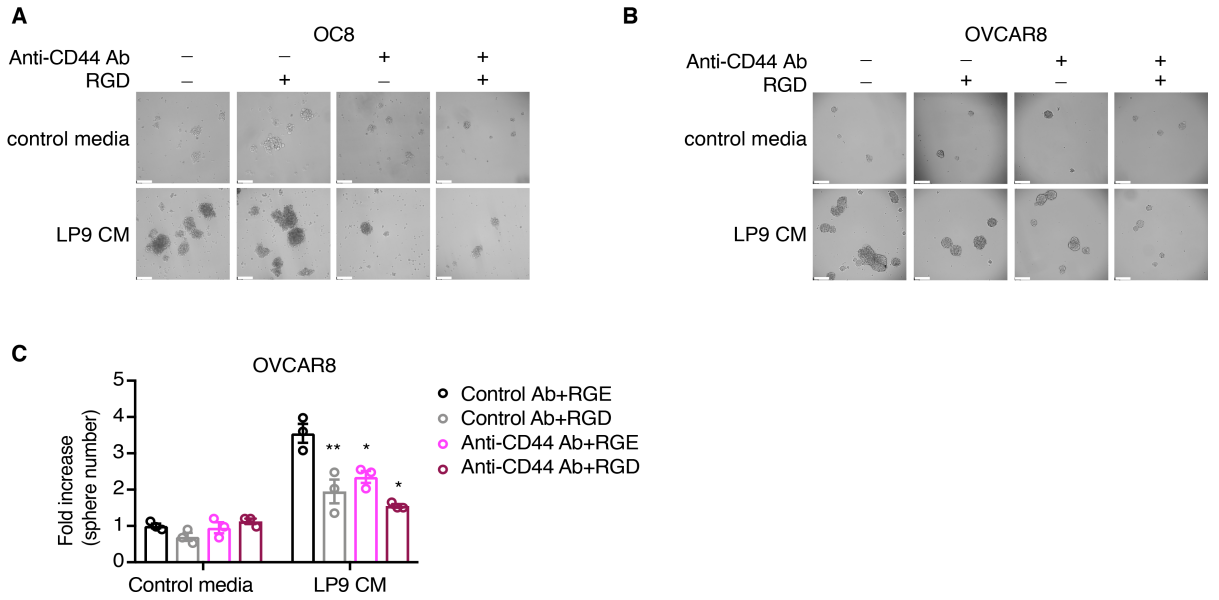

Supplemental Figure 13. CD44 receptor blockade reduces cancer associated mesothelial-induced ovarian cancer stemness. (**A)** Effect of an anti-CD44 blocking antibody, integrin-blocking RGD peptide, or their combination on LP9 CM-mediated sphere formation increase of OC8 cells. Representative images are shown. Scale bar, 200 µm. (**B-C**) Effect of an anti-CD44 blocking antibody, integrin-blocking RGD peptide, or their combination on LP9 CM-mediated sphere formation increase of OVCAR8 cells. Representative images are shown in B. Scale bar, 200 µm. Quantification of fold increase is shown in C (n=3; mean ± SEM; *p<0.05, **p<0.01 versus LP9 CM + control Ab + RGE; two-way ANOVA test).

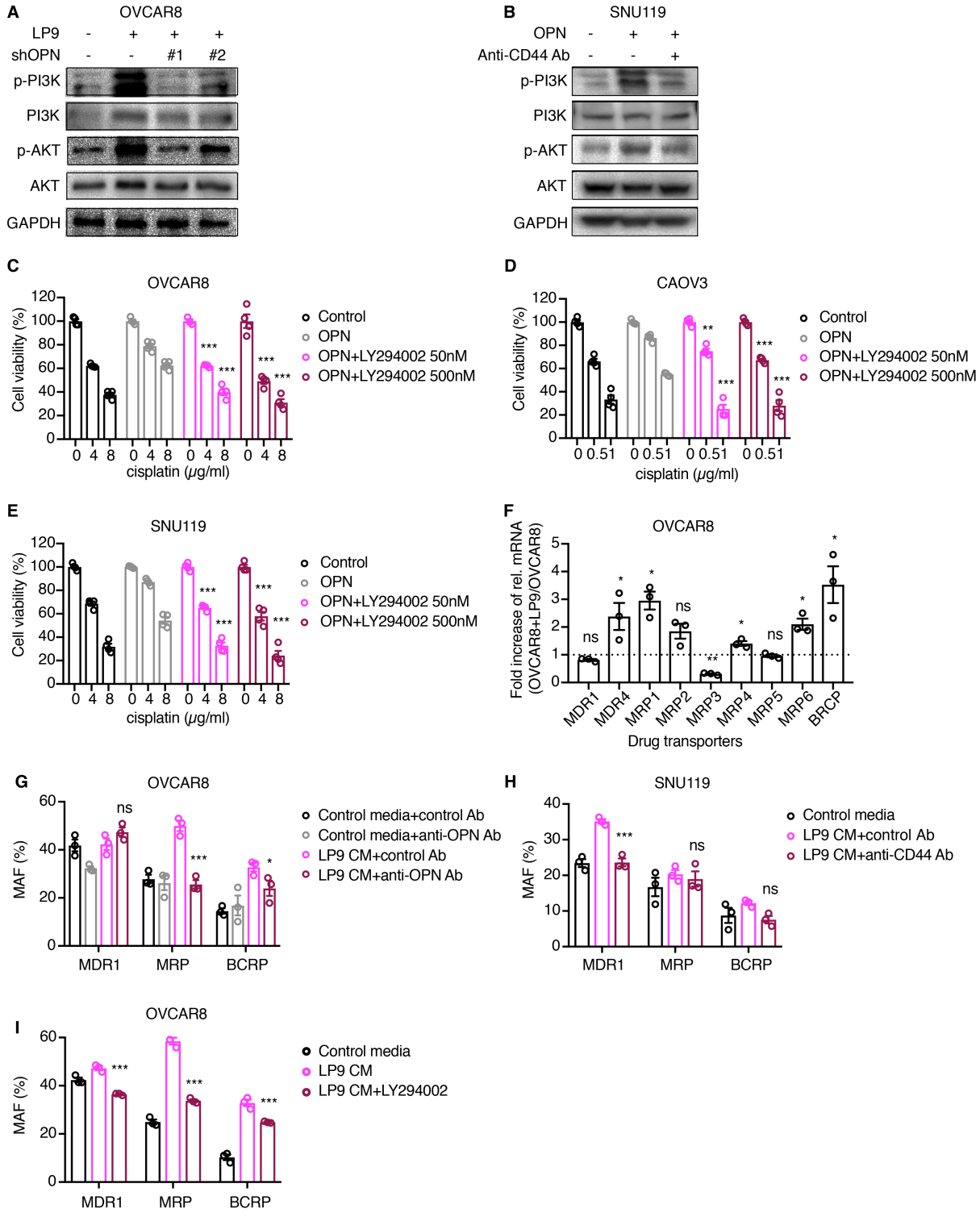

Supplemental Figure 14. Cancer associated mesothelial cells promotes ovarian cancer chemoresistance through osteopontin, PI3K-AKT signaling and ABC transporter activity.
(**A**) Western blot analysis of PI3K-AKT pathway in OVCAR8 cells co-cultured with LP9 shControl or LP9 shOPN cells. **(B)** Western blot analysis of PI3K-AKT pathway in SNU119 cells treated with exogenous OPN and/or anti-CD44 blocking antibody. (**C-E**) Effect of PI3K-AKT pathway inhibitor LY294002 on

exogenous OPN-mediated cisplatin resistance of OVCAR8, CAOV3 or SNU119 cells (n=4; mean ± SEM; **p<0.01, ***p<0.001 versus exogenous OPN; two-way ANOVA test). (**F**) Fold increase of relative mRNA expression of ABC transporters in OVCAR8 with LP9 co-culture versus OVCAR8 monoculture, as normalized to *GAPDH* mRNA in real-time PCR analysis (n=3; mean ± SEM; *p<0.05, **p<0.01, ns, not significant; two-tailed Student's t-test). (**G-I**) EFLUXX-ID® Green multidrug resistance assay by flow cytometry detecting the activities of three major types of ABC transporters (MDR1, MRP and BCRP) in OVCAR8 cells treated with LP9 conditioned media (CM) and/or anti-OPN blocking antibody (G); in SNU119 cells treated with LP9 CM and/or anti-CD44 blocking antibody (H); and in OVCAR8 cells treated with LP9 CM and/or PI3K-AKT pathway inhibitor LY294002 (I). Multidrug resistance activity factor (MAF) indicative of corresponding ABC protein activity is shown (n=3; mean ± SEM; *p<0.05, ***p<0.001 versus LP9 CM or LP9 CM + control Ab, ns, not significant; two-way ANOVA test).

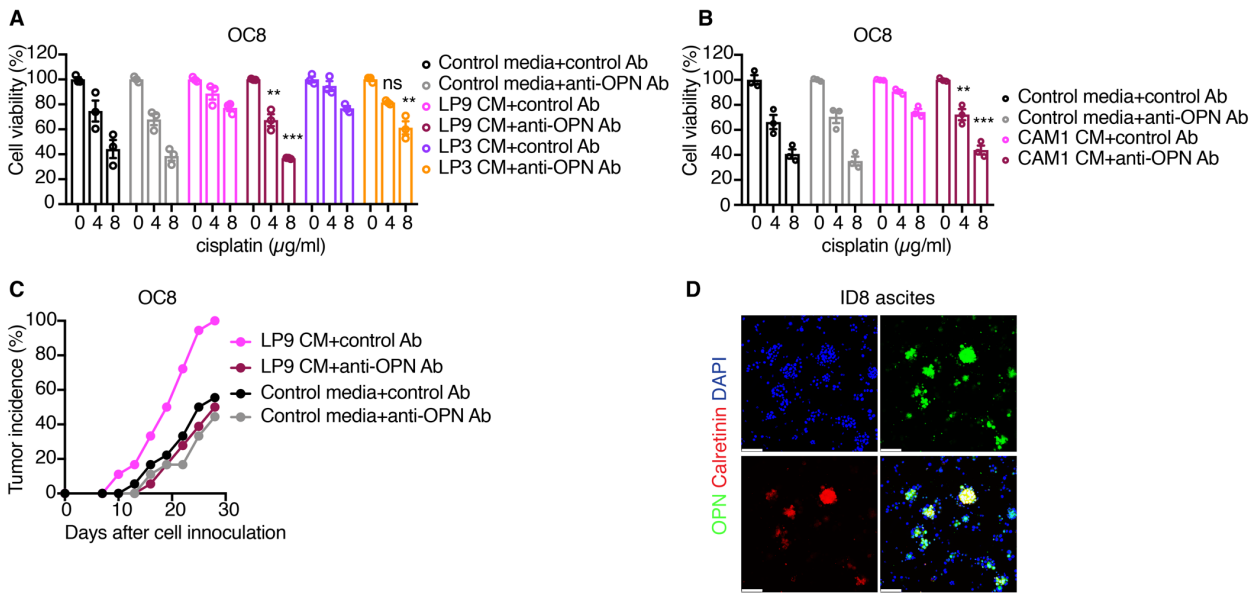

Supplemental Figure 15. An anti-OPN neutralizing antibody reduces cancer associated mesothelial cell mediated ovarian cancer chemoresistance.

(**A**) Effect of an anti-OPN neutralizing antibody or control antibody on LP9 or LP3 conditioned media (CM)-mediated OC8 resistance to cisplatin (n=3; mean ± SEM; **p<0.01, ***p<0.001 versus LP9 or LP3 CM + control Ab; ns, not significant; two-way ANOVA test). (**B**) Effect of an anti-OPN neutralizing antibody or control antibody on CAM1 CM-mediated OC8 resistance to cisplatin (n=3; mean ± SEM; **p<0.01, ***p<0.001 versus CAM1 CM + control Ab; two-way ANOVA test). (**C**) Effect of preincubation with an anti-OPN antibody in the absence or presence of LP9 conditioned media (CM) on OC8 subcutaneous tumor incidence in immunodeficient mice (n=18 mice per group). (**D**) Immunofluorescence of OPN (green) and mesothelial cell marker calretinin (red) in total ascites cells from ID8 i.p. injected mice. Nuclei were stained with DAPI (blue). Scale bars: 100 μm.

Supplemental Table 1. Patient characteristics of primary isolated CAMs

CAM ID	Age	Pathology	Chemotherapy treatment	Source
CAM1	39	Recurrent Low Grade Serous Cancer	Multiple	Ascites
CAM2	72	High Grade Serous Cancer	Naive	Ascites

Supplemental Table 2. Clinicopathological information and treatment history of the ovarian cancer patients analyzed in Figure 5F.

#	Pathology	Age	Stage	Chemotherapy treatment	Calretinin+ (%) in total ascites cells
1	High grade serous adenocarcinoma	59	IIB	Chemonaive	80.81
2	High grade serous adenocarcinoma	67	IIIC	Chemonaive	41.42
3	High grade serous ovarian cancer	72	IIIC	Neoadjuvant	16.02
4	Recurrent high grade serous carcinoma	49	IIIC	Multiple	31.91
5	High grade serous carcinoma	66	IVA	Chemotherapy	34.56
6	High grade serous carcinoma	36	IVB	Chemonaive	15.68
7	High grade serous carcinoma	52	IVB	Neoadjuvant	13.97
8	High grade serous carcinoma	38	IIIB	Neoadjuvant	37.79
9	High grade serous carcinoma	71	IIIA	Neoadjuvant	8.56
10	High grade serous carcinoma	71	IIIC	Chemonaive	10.92
11	High grade serous carcinoma	63	IIIC	Chemonaive	21.51
12	High grade serous carcinoma	52	IIIC	Chemonaive	23.01
13	High grade serous carcinoma	70	IIIC	Neoadjuvant	8.61
14	Endometrial adenocarcinoma	69	IIIC	Neoadjuvant	16.23

Supplemental Table 3. Chemicals, drugs and reagents in this study

Chemicals, Drugs and Reagents	Source	Identifier
Proteinase K	Thermo Fisher Scientific	Cat# 25530049
RGD	Abcam	Cat# ab142698
RGE(S)	Sigma Aldrich	Cat# A5686
Alexa Fluor 647 phalloidin	Thermo Fisher Scientific	Cat# A22287
DAPI	Sigma Aldrich	Cat# D9542
Matrigel	Corning	Cat# 356237
Cultrex	Trevigen	Cat# 3533-001-02
GlutaMAX	Gibco	Cat# 35050061
Poly-L-lysine	Sigma Aldrich	Cat# P4707
B27	Invitrogen	Cat# 425305
Insulin	Sigma Aldrich	Cat# 91077C
EGF	Thermo Fisher Scientific	Cat# PHG0313
EGF	Peprotech	Cat# AF-100-15
Penicillin-Streptomycin-Glutamine	Thermo Fisher Scientific	Cat# 10378016
HEPES	Thermo Fisher Scientific	Cat# 15630080
CHIR99021	Cayman Chemical	Cat# 13122
B27 minus vitamin A	Gibco	Cat# Gibco 12587010
SB-202190	Peprotech	Cat# 1523072
N-Acetylcysteine	Sigma Aldrich	Cat# A9165
Nicotinamide	Sigma Aldrich	Cat# N0636
Normocin	Invivogen	Cat# ant-nr-1
FGF-basic	Sigma Aldrich	Cat# F0291
A83-01	Sigma Aldrich	Cat# SML0788
FGF-10	Peprotech	Cat# 100-26
FGF-basic	Peprotech	Cat# 100-18B
Y27632	STEMCELL Technologies	Cat# 72302
Sytox™ Blue	Biolegend	Cat# 425305
Cisplatin	WG Critical Care	Cat# 44567-511-01
Carboplatin	Teva Parenteral Medicines	Cat# 0703-4244-01
Paclitaxel	Teva Parenteral Medicines	Cat# 0703-4766-01
LY294002	Cell Signaling Technologies	Cat#9901S
TGFβ1	Peprotech	Cat#100-21
SB431542	EMD Millipore	Cat#616461

Supplemental Table 4. Antibodies used in this study

Antibody	Source	Identifier
Rabbit Anti-EpCAM Antibody [EPR677(2)]	Abcam	Cat# ab124825; RRID:AB_10973714
Mouse Anti-FSP1 Antibody Clone 1481	Novus Biologicals	Cat# NBP2-53178
Mouse Anti-vimentin Monoclonal Antibody (J144)	Thermo Fisher Scientific	Cat# MA3-745, RRID:AB_326285
Rabbit Anti-CD31 Antibody	Abcam	Cat# ab28364, RRID:AB_726362
Mouse Anti-CD45 Antibody (2D1)	Thermo Fisher Scientific	Cat# 11-9459-42, RRID:AB_1907394
Rabbit Anti-cytokeratin 8 Antibody [EP1628Y]	Abcam	Cat# ab53280; RRID:AB_869901
Mouse Anti-calretinin Antibody (Z11-E3)	Invitrogen	Cat# 180291
Rabbit Anti-osteopontin Antibody	Abcam	Cat# 8848, RRID:AB_306566
Rabbit Anti-cleaved caspase 3 Antibody	Cell Signaling Technologies	Cat# 9661, RRID:AB_2341188
Rabbit Anti-caspase 3 Antibody	Cell Signaling Technologies	Cat# 9662, RRID:AB_331439
Rabbit Anti-GAPDH Antibody (D16H11)	Cell Signaling Technologies	Cat# 5174, RRID:AB_10622025
Rabbit Anti-ERK1/2 Antibody (137F5)	Cell Signaling Technologies	Cat# 4695, RRID:AB_390779
Rabbit Anti-phospho-ERK1/2 Antibody (20G11)	Cell Signaling Technologies	Cat# 4376, RRID:AB_331772
Rabbit Anti-phospho-STAT3 Antibody (D3A7)	Cell Signaling Technologies	Cat# 9145, RRID:AB_2491009
Rabbit Anti-STAT3 Antibody (79D7)	Cell Signaling Technologies	Cat# 4904, RRID:AB_331269
Rabbit Anti-PARP Antibody	Cell Signaling Technologies	Cat# 9542, RRID:AB_2160739
Rabbit Anti-Akt Antibody	Cell Signaling Technologies	Cat# 9272, RRID:AB_329827
Rabbit Anti-phospho-Akt Antibody	Cell Signaling Technologies	Cat# 9271, RRID:AB_329825
Mouse Anti-PI3K Antibody Clone 4	BD	Cat# 610045, RRID:AB_397459
Rabbit Anti-phospho-PI3K Antibody	Cell Signaling Technologies	Cat# 4228, RRID:AB_659940
Anti-mouse IgG, HRP-linked Antibody	Cell Signaling Technologies	Cat# 7076, RRID:AB_330924
Anti-rabbit IgG, HRP-linked Antibody	Cell Signaling Technologies	Cat# 7074, RRID:AB_2099233
Mouse Anti-ALDH1A1 Antibody (H-4)	Santa Cruz	Cat# sc-374076, RRID:AB_10916407
Rat Anti-CD44 Antibody (Hermes-1)	Bioxcell	Cat# BE0262, RRID:AB_2687741
Rat IgG2a Isotope Control Antibody	Bioxcell	Cat# BE0089, RRID:AB_1107769
Rabbit Wide Spectrum Anti-cytokeratin Antibody	Abcam	Cat# ab9377, RRID:AB_307222
Rat Anti-cytokeratin 8 Antibody	DSHB	Cat# TROMA-I, RRID:AB_531826

Rabbit Anti-Phospho-Histone H2A.X Antibody	Cell Signaling Technologies	Cat# 9718, RRID:AB_2118009
Anti-rabbit Alexa Fluor 488 Secondary Antibody	Thermo Fisher Scientific	Cat# A-11008, RRID:AB_143165
Anti-rat Alexa Fluor 647 Secondary Antibody	Thermo Fisher Scientific	Cat# A-21247, RRID:AB_141778
Anti-rat Alexa Fluor 546 Secondary Antibody	Thermo Fisher Scientific	Cat# A-11081, RRID:AB_2534125
Anti-rabbit Alexa Fluor 647 Secondary Antibody	Thermo Fisher Scientific	Cat# A-21245, RRID:AB_2535813
Anti-rat Alexa Fluor 594 Secondary Antibody	Thermo Fisher Scientific	Cat# A-11007, RRID:AB_10561522
Anti-rabbit Alexa Fluor 594 Secondary Antibody	Thermo Fisher Scientific	Cat# A-11012, RRID:AB_2534079
Anti-rat Alexa Fluor 488 Secondary Antibody	Thermo Fisher Scientific	Cat# A-21208, RRID:AB_2535794
Anti-mouse Alexa Fluor 647 Secondary Antibody	Thermo Fisher Scientific	Cat# A-31571, RRID:AB_162542
Anti-mouse Alexa Fluor 488 Secondary Antibody	Thermo Fisher Scientific	Cat# A-21202, RRID:AB_141607
Anti-rabbit Alexa Fluor 555 Secondary Antibody	Thermo Fisher Scientific	Cat# A-21428, RRID:AB_2535849
Goat Anti-osteopontin Antibody	R&D	Cat# AF1433, RRID:AB_354791
Goat IgG Control Antibody	R&D	Cat# AB-108-C, RRID:AB_354267
Mouse Anti-H-2Kd PE Antibody Clone SF1-1.1	BD	Cat# BDB562004
Mouse Anti-EpCAM Antibody Clone 1B7	Thermo Fisher Scientific	Cat# 50-9326-42, RRID:AB_10598658
Rat Anti-cisplatin-DNA Antibody Clone CP9/19	Abcam	Cat# 103261, RRID:AB_10715243
Rabbit Anti-calretinin Antibody (SP13)	Thermo Fisher Scientific	Cat# MA5-14540, RRID:AB_10985167
Goat Anti-osteopontin Antibody	Novus Biologicals	Cat# NB100-1883, RRID:AB_10000967

Supplemental Table 5. Primers for real-time PCR analysis

Gene Symbol	Forward Primer (5'- 3')	Reverse Primer (5'- 3')
ALDH1A1	CACGCCAGACTTACCTGTCC	TCCTCCTCAGTTGCAGGATT
OCT3/4	TTCAGCCAAACGACCATCTG	GAACCACACTCGGACCACATC
SOX2	CACACTGCCCCTCTCACACAT	CCCATTTCCCTCGTTTTTCTT
NANOG	CACCAGTCCCAAAGGCAAAC	GCCTTCTGCGTCACACCATT
OPN	AGAAGTTTCGCAGACCTGACA	AACGGGGATGGCCTTGTATG
CD44	CCAATGCCTTTGATGGACCA	TGTGAGTGTCCATCTGATTC
MDR1	GCCTGGCAGCTGGAAGACAAATAC	CCATACCAGAAGGCCAGAGCATAA
MDR4	TGGCCCTGGTTGGAAGTAGTG	AGAAGGATCTTGGGGTTGCGAA
MRP6	CACTGCGCTCCAGGATCAGC	CAGACCAGGCCTGACTCCTG
MRP5	AGAGGTGACCTTTGAGAACGCA	CTCCAGATAACTCCACCAGACGG
MRP4	TTCAGTGTGCTGGGATGAGGT	TCAGTGATGAGAACAACTTCC
MRP3	GCTCAAGATGGTCCTGGGTGT	CAGGGCAAAGTGGATGTAGAA
MRP2	GGGAAGTTGATGAAGAGATGA	GGAATGATTTCAGGAGCACCA
MRP1	AGTGGAACCCCTCTCTGTTTAAG	CCTGATACGTCTTGGTCTTCATC
BRCP	TACCTGTATAGTGTACTTCAT	GGTCATGAGAAGTGTTGCT

Supplemental Video 1. 3D rendering of ovarian cancer organoids formed with CAM CM.

A volume rendering of a confocal fluorescence/coherent anti-Stokes Raman scattering (CARS) 3D microscopy image covering a volume of 91x91x36.5 µm (voxel size: 0.089x0.089x0.5 µm), visualizing the cellular build-up and external/luminal composition of a 27-day human ovarian cancer organoid with a diameter of 73 µm. At this stage, the cells represented by their nuclei (DAPI, blue) display a highly polarized organization of their components. While their F-actin network (Alexa Fluor 647, magenta) and intracellular lipid stores (CARS, yellow) face the luminal side of the organoid, the stem cell marker ALDH1A1 (Alexa Fluor 546, red) is organized between the cells and on the external side. The organoid was optically - not physically – sectioned.